

Transformation of One-dimensional Achiral Structure to Three-dimensional Chiral Structure: Mechanistic Study and Catalytic Activities of Chiral Structure

Purna Chandra Rao,^a Sonu Pratap Chaudhary,^a Denis Kuznetsov^b and Sukhendu Mandal^{a*}

^a School of Chemistry

Indian Institute of Science Education and Research Thiruvananthapuram, Thiruvananthapuram, Kerala, India, 695016

*E-mail: sukhendu@iisertvm.ac.in

^b National University of Science and Technology “MISIS”, Department of Functional Nano systems and High temperature Materials, Leninsky pr.4, Moscow, Russia, 119049

Supporting Information

General experimental procedure for catalysis

(a) Regio- and chemo-selective Enamination reaction:

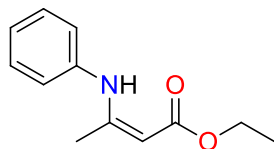
In this catalytic reaction, various amines (2 mmol), β -keto ester (2 mmol) and catalyst **2'** (0.1 mmol, 40.9 mg, 5 mol %), was taken in a reaction flask. The reaction was conducted at room temperature under solvent-free conditions and N₂ atmosphere at the appropriate time (hours) to give the expected product with excellent yields. After the reaction, the resultant mixture was diluted with water and filtered off the catalyst. Then extracted the aqueous layer with ethyl acetate (10 mL) three times. The separated organic layer was dried over anhydrous sodium sulphate, and then the solvent was removed under vacuum. Finally, the expected product was purified by column chromatography over the silica-gel using ethyl acetate/pet ether as an eluent. All the compounds were characterized by ¹H NMR studies and all were matching with previously reported data. The recovered catalyst was washed with methanol several times, dried and then reused for the next cycle.

(b) 1, 3 dipolar cycloaddition (click reaction):

The click reaction with benzyl azide (2 mmol), phenyl acetylene (2 mmol) and catalyst **2'** (0.1 mmol, 40.9 mg, 5 mol %) under solvent-free conditions at room temperature for 6 h under N₂ atmosphere. The above procedure was used for extraction and purification of the product. The results have given 1, 4 substituted triazole as a major product with excellent yield. The ¹H NMR spectra match with previously reported data.

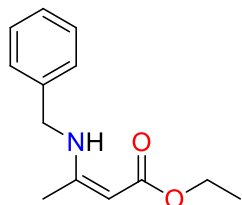
¹H NMR spectra of Enamine reaction products and click product

1. (Z)-ethyl 3-(phenylamino) but-2-enoate:



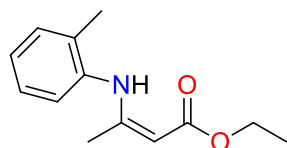
¹H NMR (500 MHz, CDCl₃) δ/ppm 10.40 (br s, 1H), 7.35-7.32 (m, 2H), 7.18-7.09 (m, 3H), 4.71 (s, 1H), 4.17 (q, *J* = 5 Hz, 1H), 2.01 (s, 3H), 1.31 (t, *J* = 5 Hz, 3H). All spectral data match those previously reported.

2. (Z)-ethyl 3-(benzylamino) but-2-enoate:



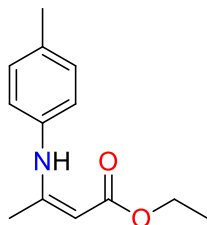
¹H NMR (500 MHz, CDCl₃) δ/ppm 8.96 (br s, 1H), 7.37-7.27 (m, 5H), 4.55 (s, 1H), 4.44 (d, *J* = 5 Hz, 2H), 4.12 (q, *J* = 10 Hz, 2H), 1.93 (s, 3H), 1.27 (t, *J* = 10 Hz, 3H). All spectral data match those previously reported.

3. (Z)-ethyl 3-(o-tolylamino) but-2-enoate:



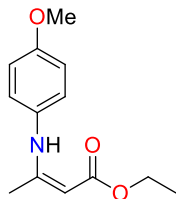
¹H NMR (500 MHz, CDCl₃) δ/ppm 10.05 (br s, 1H), 7.15-6.99 (m, 4H), 4.62 (s, 1H), 4.08 (q, *J* = 10 Hz, 2H), 2.21 (s, 3H), 1.78 (s, 3H), 1.21 (t, *J* = 10 Hz, 3H). All spectral data match those previously reported.

4. (Z)-ethyl 3-(p-tolylamino) but-2-enoate:



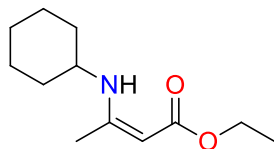
¹H NMR (500 MHz, CDCl₃) δ/ppm 10.29 (br s, 1H), 7.14 (d, *J* = 10 Hz, 2H), 6.99 (d, *J* = 5 Hz, 2H), 4.68 (s, 1H), 4.16 (q, *J* = 5 Hz, 2H), 2.35 (s, 3H), 1.97 (s, 3H), 1.30 (t, *J* = 10 Hz, 3H). The spectral data match those previously reported.

5. (Z)-ethyl 3-((4-methoxyphenyl) amino) but-2-enoate:



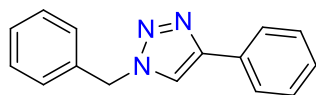
^1H NMR (500 MHz, CDCl_3) δ /ppm 10.16 (br s, 1H), 7.04 (t, $J = 5$ Hz, 2H), 6.87 (q, $J = 5$ Hz, 2H), 4.66 (s, 1H), 3.82 (s, 3H), 1.90 (s, 3H), 1.30 (t, $J = 5$ Hz, 3H). The spectral data match those previously reported.

6. (Z)-ethyl 3-(cyclohexylamino) but-2-enoate:

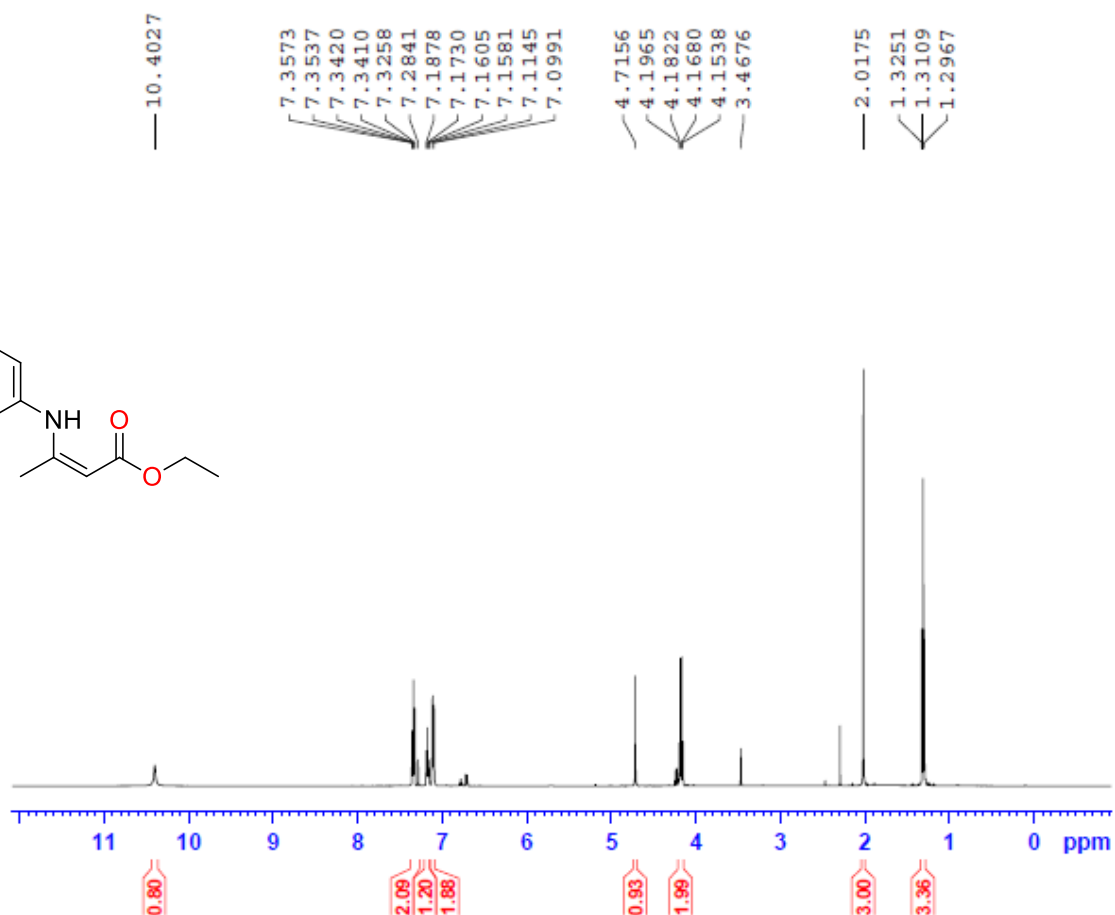
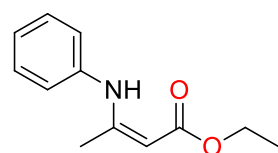


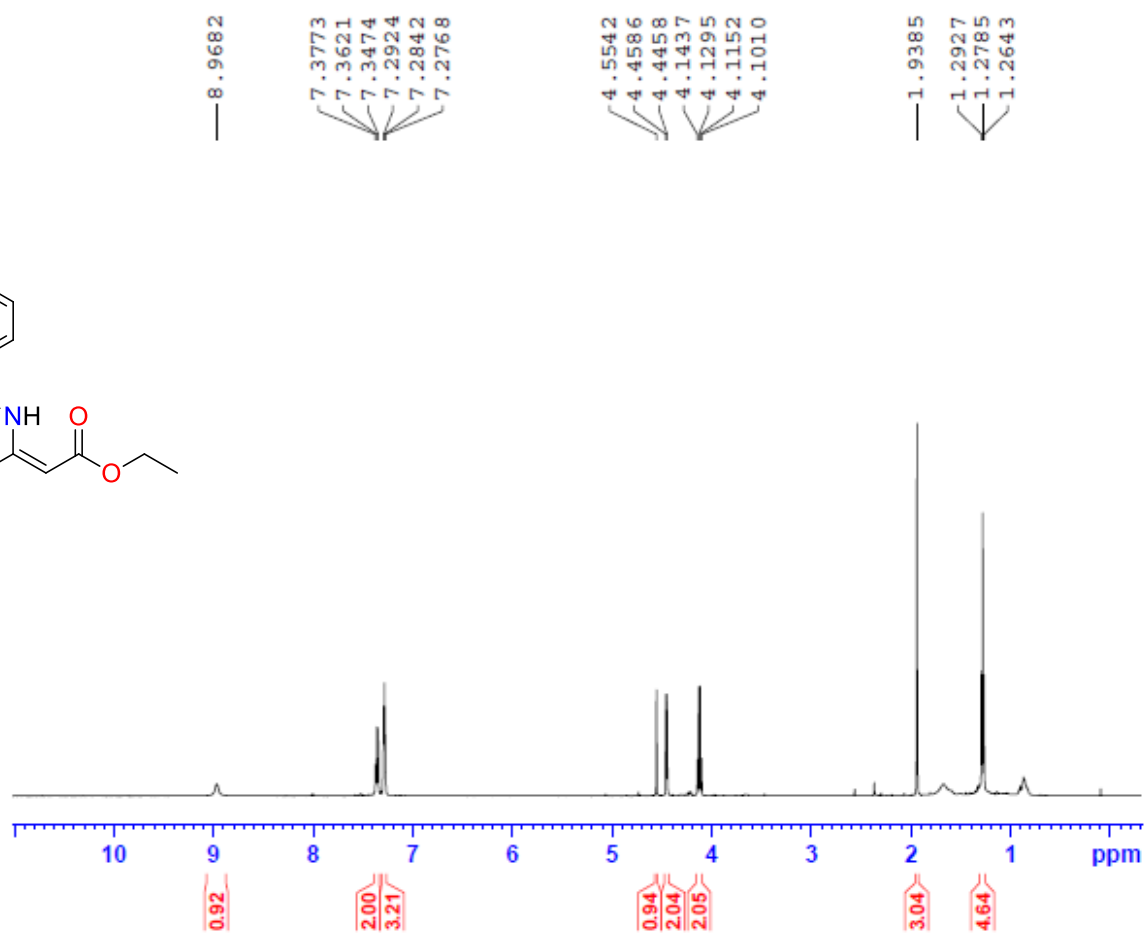
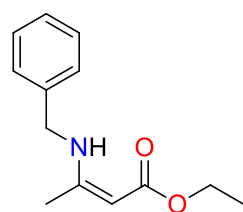
^1H NMR (500 MHz, CDCl_3) δ /ppm 8.63 (br s, 1H), 4.40 (s, 1H), 4.11-4.07 (m, 2H), 3.34-3.29 (m, 1H), 1.89 (t, $J = 25$ Hz, 3H), 1.76 (q, $J = 5$ Hz, 2H), 1.59 (d, $J = 15$ Hz, 2H), 1.33-1.27 (m, 9H). All spectral data match those previously reported.

7. 1-benzyl-4-phenyl-1H-1, 2, 3-triazole:



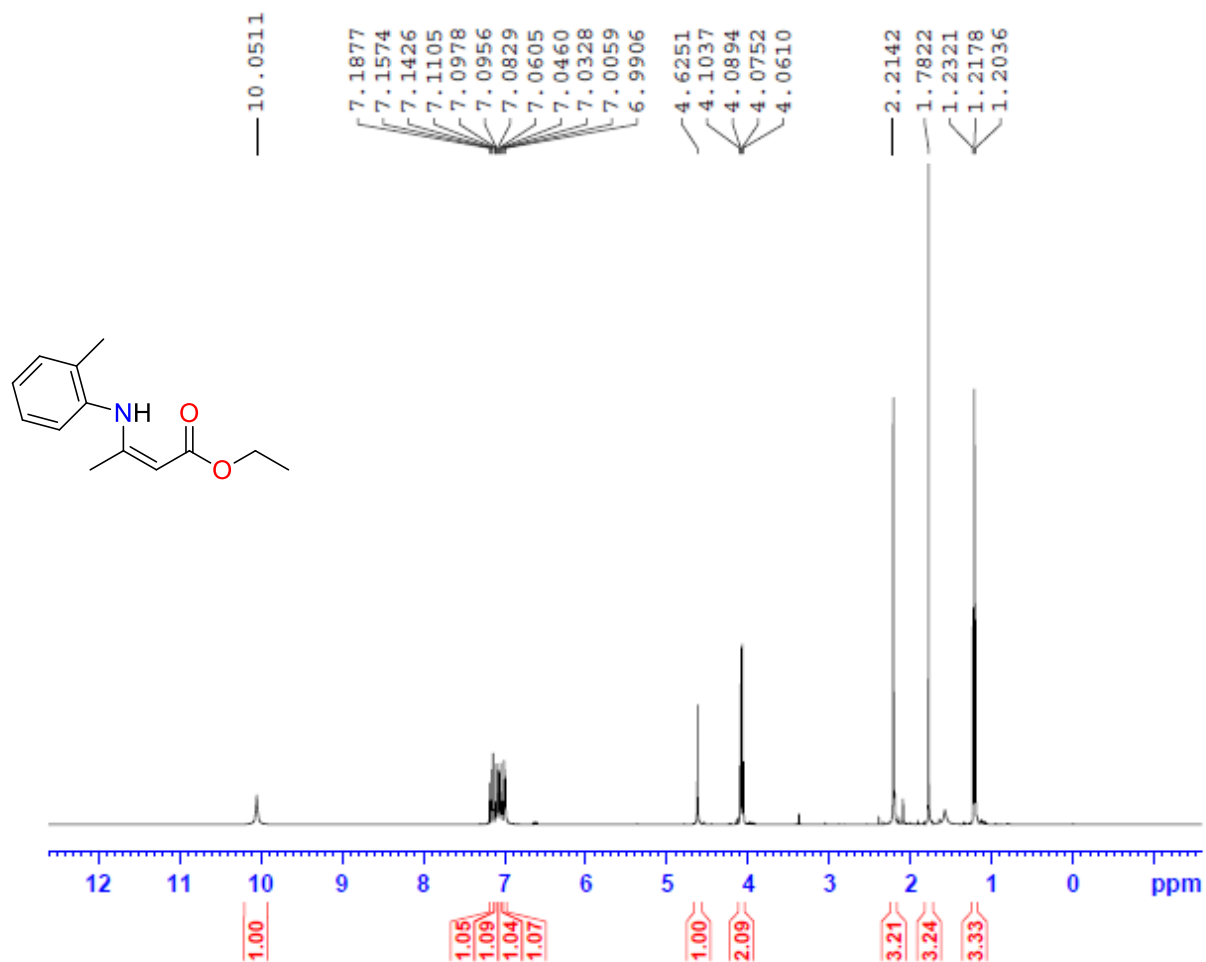
^1H NMR (500 MHz, CDCl_3) δ /ppm 7.81 (d, $J = 5$ Hz, 2H), 7.68 (s, 1H), 7.43-7.28 (m, 8H), 5.60 (s, 2H). All spectral data match those previously reported.



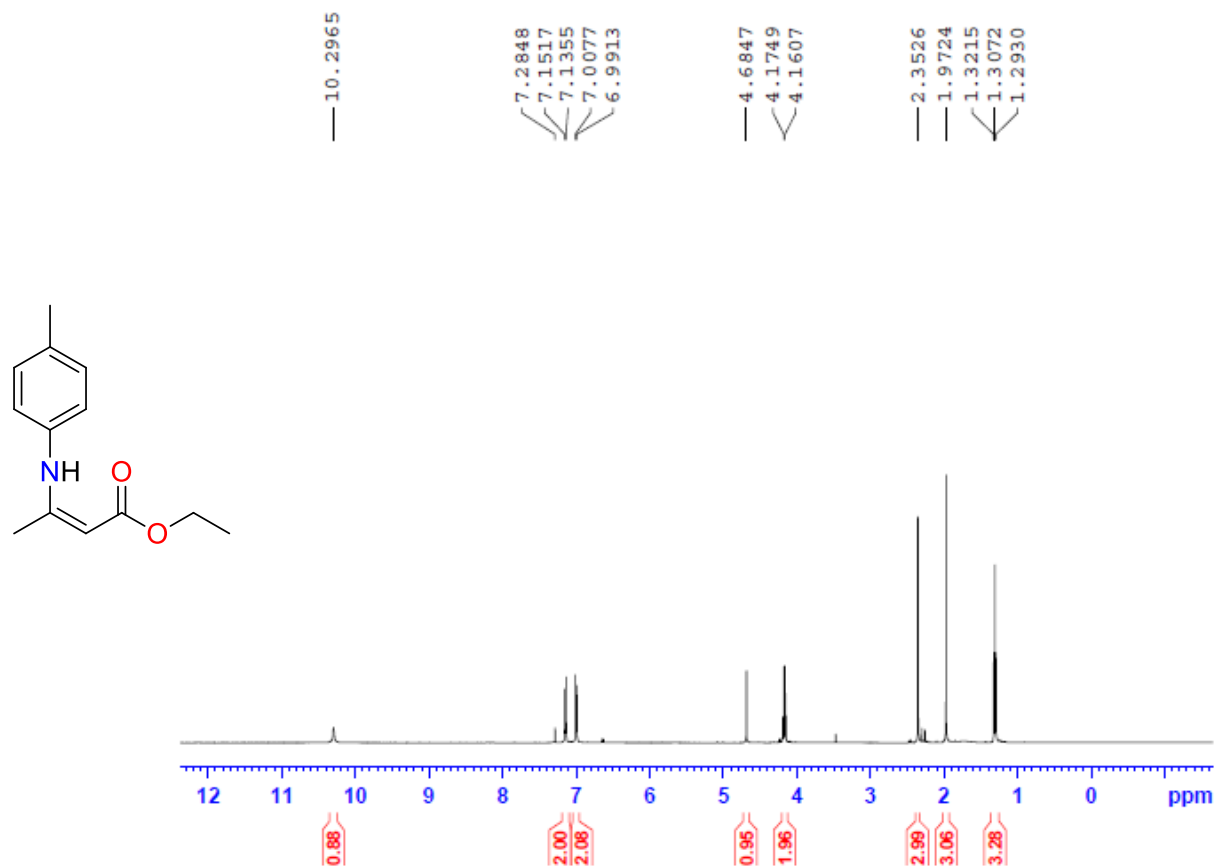


TOLUIDENE-ENAM

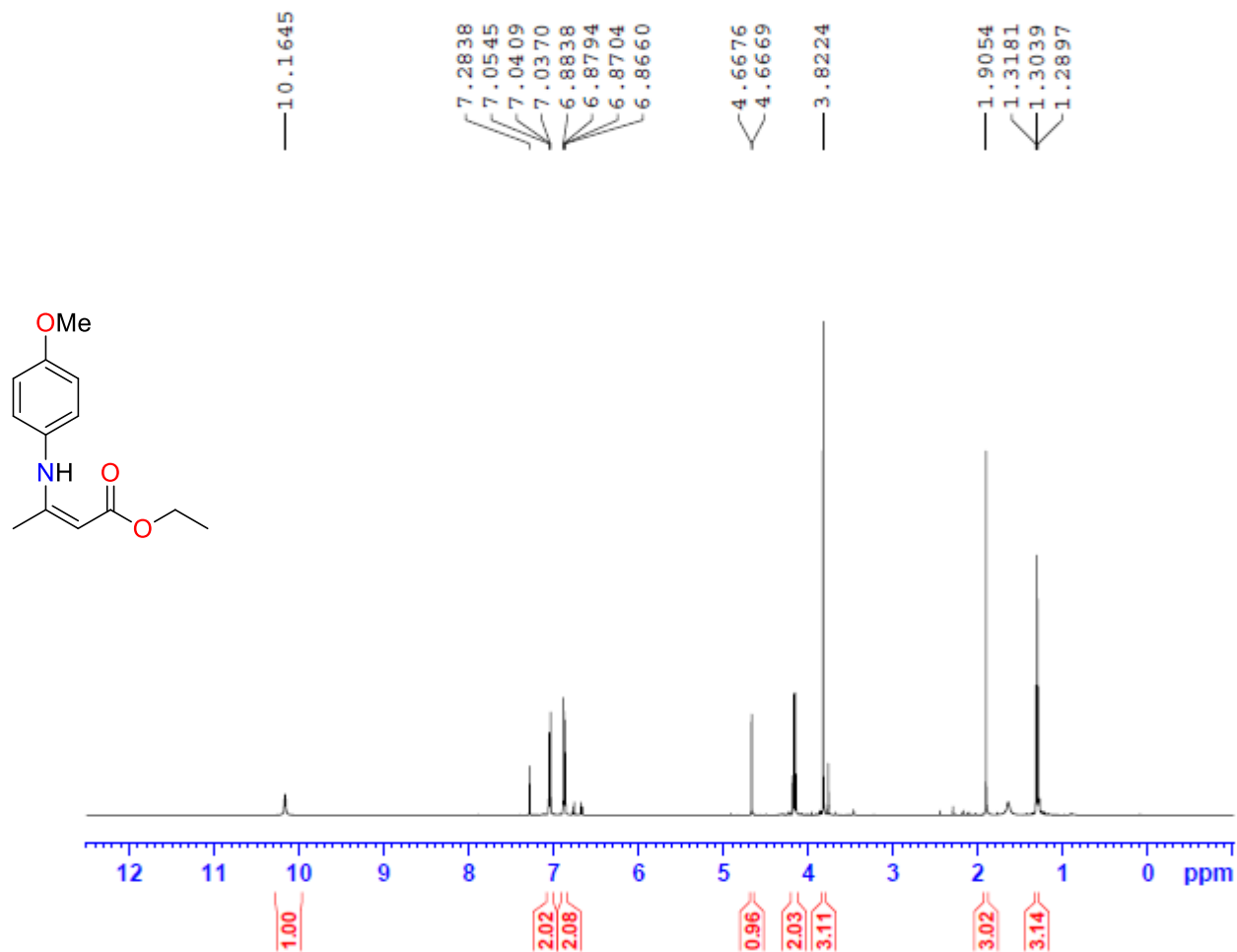
OTON CDCl3 {C:\Bruker\TopSpin3.2} nmr 51



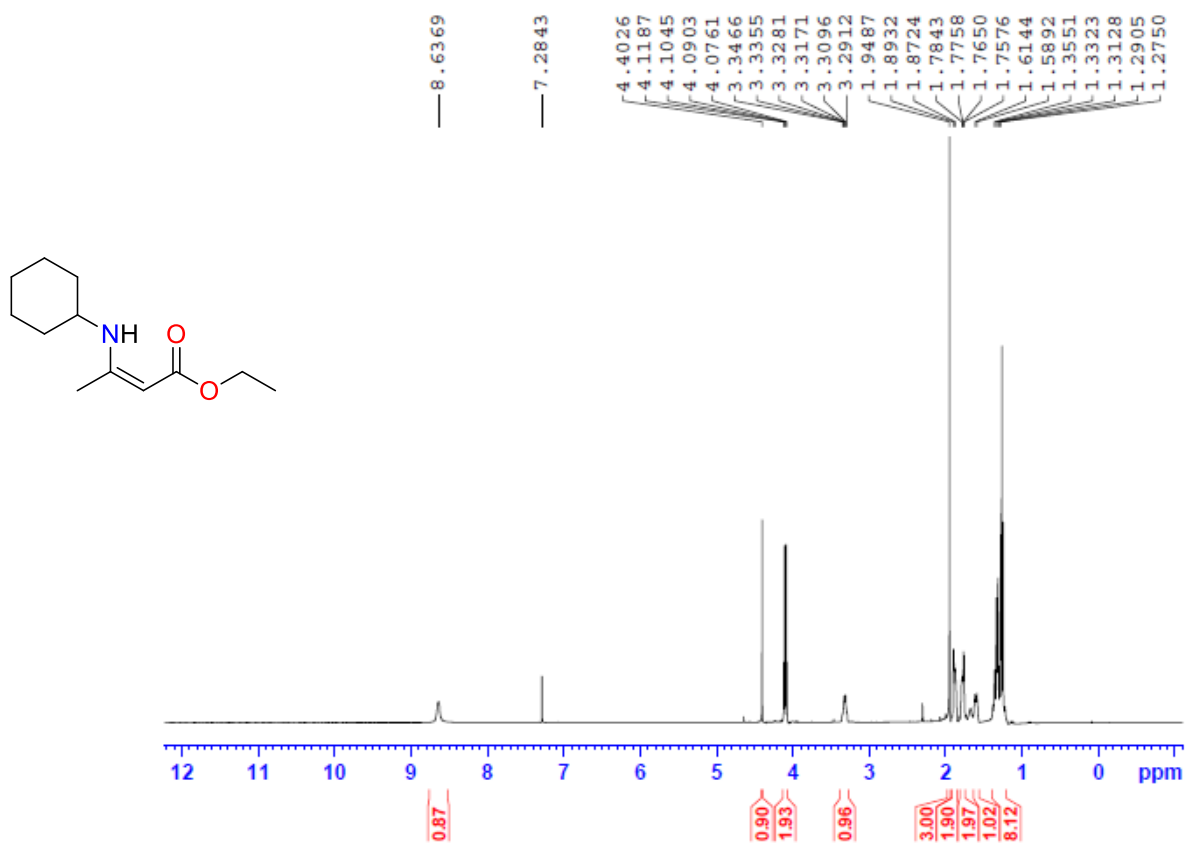
P-Toluidene-enam
 PROTON CDCl3 {C:\Bruker\TopSpin3.2} nmr 50



anisidine-enam-new
 PROTON CDCl3 {C:\Bruker\TopSpin3.2} nmr 15



cyc-ene-pure



CL-Cu-FDC

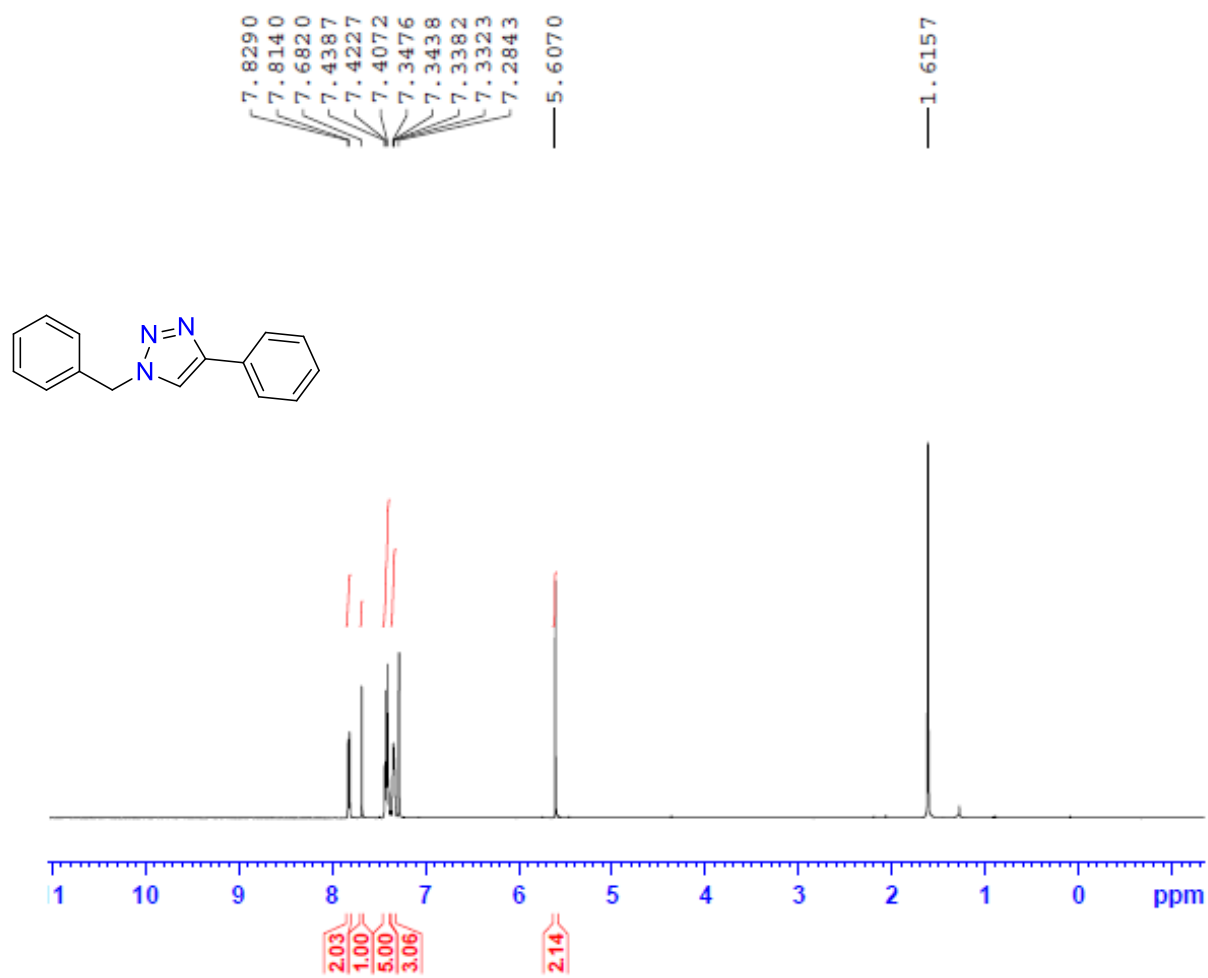


Table S1. Crystallographic parameters for compound **1**^[a]

Parameters	Compound 1
Empirical formula	C ₁₆ H ₂₂ CuN ₂ O ₁₁
Formula weight	481.89
Wavelength	0.71073 Å
Crystal System	Monoclinic
Space Group	<i>P</i> 2 ₁ / <i>c</i> (No.14)
<i>a</i> (Å)	7.0884(4)
<i>b</i> (Å)	11.1739(6)
<i>c</i> (Å)	23.9893(12)
$\alpha(^{\circ})$	90
$\beta(^{\circ})$	92.168(3)
$\gamma(^{\circ})$	90
Volume(Å ³)	1898.71(18)
<i>Z</i>	4
Calculated density (g/cm ³)	1.686
θ range ($^{\circ}$)	2.492 to 28.447
Absorption coefficient (mm ⁻¹)	1.216
Reflections collected	18026
Unique reflections	4742
Goodness-of-fit	1.038
Number of parameters	309
Final R indices [<i>I</i> > 2σ(<i>I</i>)]	<i>R</i> ₁ = 0.0317, <i>wR</i> ₂ = 0.0743
R indices (all data)	<i>R</i> ₁ = 0.0492, <i>wR</i> ₂ = 0.0803

^[a] $R_1 = \Sigma ||F_o| - |F_c|| / \Sigma |F_o|$; $wR_2 = \{ [w(F_o^2 - F_c^2)^2] / [w(F_o^2)^2] \}^{1/2}$; $w = 1 / [\sigma^2(F_o)^2 + (aP)^2 + bP]$; $P = [\max(F_o^2, 0) + 2(F_c^2)]/3$, where $a = 0.0369$ and $b = 0.6267$ for compound **1**.

Table S2. Selected bond length for compound **1**.

Moiety	Bond lengths (Å)
Cu(1)-O(2)	1.958 (2)
Cu(1)-O(1)	1.981 (2)
Cu(1)-N(1)	2.033 (2)
Cu(1)-N(2)	2.042 (2)
Cu(1)-O(3)	2.422 (2)
Cu(1)-O(4)	2.430 (2)

Table S3. Crystallographic parameters for compound **2**^[b]

Parameters	Compound 2
Empirical formula	C ₁₆ H ₁₃ CuN ₂ O ₇
Formula weight	408.82
Wavelength	0.71073 Å
Crystal System	Hexagonal
Space Group	<i>P</i> 6 ₅ (NO.170)
<i>a</i> (Å)	11.0550(2)
<i>b</i> (Å)	11.0550(2)
<i>c</i> (Å)	47.6676(10)
$\alpha(^{\circ})$	90
$\beta(^{\circ})$	90
$\gamma(^{\circ})$	120
Volume(Å ³)	5045.1 (2)
<i>Z</i>	6
Calculated density (g/cm ³)	1.615
θ range ($^{\circ}$)	3.015 to 26.364
Absorption coefficient (mm ⁻¹)	1.341
Reflections collected	26345
Unique reflections	6847
Goodness-of-fit	1.105
Number of parameters	478
Final <i>R</i> indices [<i>I</i> >2σ(<i>I</i>)]	<i>R</i> 1 = 0.0426, <i>wR</i> 2 = 0.0897
<i>R</i> indices (all data)	<i>R</i> 1 = 0.0477, <i>wR</i> 2 = 0.0916

^[b] $R_1 = \Sigma ||F_o| - |F_c|| / \Sigma |F_o|$; $wR_2 = \{ [w(F_o^2 - F_c^2)^2] / [w(F_o^2)^2] \}^{1/2}$; $w = 1 / [\sigma^2(F_o)^2 + (aP)^2 + bP]$; $P = [\max(F_o^2, 0) + 2(F_c^2)]/3$, where $a = 0.0254$ and $b = 5.0400$ for compound **2**.

Table S4. Selected bond length for compound **2**.

Moiety	Bond lengths (Å)
Cu(1)-O(1)	1.974 (5)
Cu(1)-O(3)	1.951 (5)
Cu(1)-O(4)	2.380 (7)
Cu(1)-N(4)	1.992 (5)
Cu(1)-N(3)	2.008 (5)

Table S5. Structural determination of four different crystals form four different reaction vials after solvo-thermal syntheses for compound **2**.

Expt. No.	a	b	c	R	Flack parameter	Goodness – of-Fit (F^2)
1.	11.0550(2)	11.0550(2)	47.6676(10)	0.0403	0.037 (5)	1.003
2.	11.0575(6)	11.0575(6)	47.773(3)	0.0788	0.007 (10)	0.963
3.	11.0558(4)	11.0558(4)	47.7877(18)	0.0999	0.07 (4)	1.077
4.	11.0575(6)	11.0575(6)	47.773(3)	0.0543	0.003 (10)	0.932

Table S6: Comparative study of catalytic effect with standard catalysts^a

Product^b	Catalyst	Catalyst loading	time	Yield (%)	Reference
1	Sc(OTf) ₃	5 mol%	1 h	94	1
1	Compound 2	5 mol%	2 h	92	Present work
2	InBr ₃	1 mol%	50 min	98	2
2	MgSO ₄	Mg: 10 mol%	48 h	57	3
2	Zn(OAc) ₂ .2H ₂ O	Zn: 5 mol%	48 h	57	3
2	Compound 2	5 mol%	1 h	95	Present work
4	InBr ₃	1 mol%	1.5 h	92	2
4	Compound 2	5 mol%	3 h	88	Present work
5	Sc(OTf) ₃	5 mol%	2.5 h	90	1
5	InBr ₃	1 mol%	45 min	90	2
5	Compound 2	5 mol%	2 h	92	Present work

^aThese standard catalysts are homogeneous in nature while our as-synthesize catalyst is heterogeneous.

^bThe products number are based on Table 1 in the main manuscript.

TOPOLOGICAL REPRESENTATION OF COMPOUND 2

#####

1:C32 H26 Cu2 N4 O14

#####

Topology for Cu1

Atom Cu1 links by bridge ligands and has

Common vertex with	R (A-A)	f
Cu 1 -0.0702 0.4476 0.9500 (-1 0 0)	9.812A	1
Cu 1 0.5524 1.4822 0.6167 (1 1-1)	9.812A	1
Cu 1 1.4822 0.9298 0.7833 (1 0 0)	11.055A	1
Cu 1 -0.5178 0.9298 0.7833 (-1 0 0)	11.055A	1

Topology for Cu2

Atom Cu2 links by bridge ligands and has

Common vertex with	R (A-A)	f
Cu 2 -0.4938 0.4201 0.8671 (-1 0 0)	9.951A	1
Cu 2 0.5799 1.0861 0.5338 (1 1-1)	9.951A	1
Cu 2 0.0861 -0.4938 0.7005 (0-1 0)	11.055A	1
Cu 2 0.0861 1.5062 0.7005 (0 1 0)	11.055A	1

Structural group analysis

Structural group No 1

Structure consists of 3D framework with CuO₆N₂C₁₆H₁₂

Coordination sequences

Cu1: 1 2 3 4 5 6 7 8 9 10

Num 4 12 36 72 122 188 264 354 456 570

Cum 5 17 53 125 247 435 699 1053 1509 2079

TD10=2079

Vertex symbols for selected sublattice

Cu1 Point symbol: {7⁵.9}

Extended point symbol: [7(2).9(2).7(3).7(3).7(3).7(3)]

Point symbol for net: {7⁵.9}

4-c net; uninodal net

Topological type: qzd quartz-dual, "dense" net (topos&RCSR.ttd) {7⁵.9} - VS
[7(2).*.7(3).7(3).7(3).7(3)] (16813 types in 3 databases)

Structural group No 2

Structure consists of 3D framework with CuO₆N₂C₁₆H₁₂

Coordination sequences

Cu2: 1 2 3 4 5 6 7 8 9 10

Num 4 12 36 72 122 188 264 354 456 570

Cum 5 17 53 125 247 435 699 1053 1509 2079

TD10=2079

Vertex symbols for selected sublattice

Cu2 Point symbol: {7⁵.9}

Extended point symbol: [7(2).9(2).7(3).7(3).7(3).7(3)]

Point symbol for net: {7⁵.9}

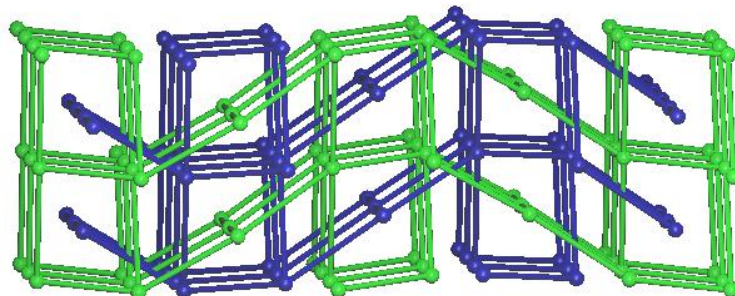
4-c net; uninodal net

Topological type: qzd quartz-dual, "dense" net (topos&RCSR.ttd) {7⁵.9} - VS
[7(2).*.7(3).7(3).7(3).7(3)] (16813 types in 3 databases)

Totally 2(1+1) interpenetrating nets

Elapsed time: 11.00 sec.

Topology of compound 2:



(a) Along 100 projection

Characterization of compounds 1 and 2

(a) Powder X-ray diffraction (PXRD)

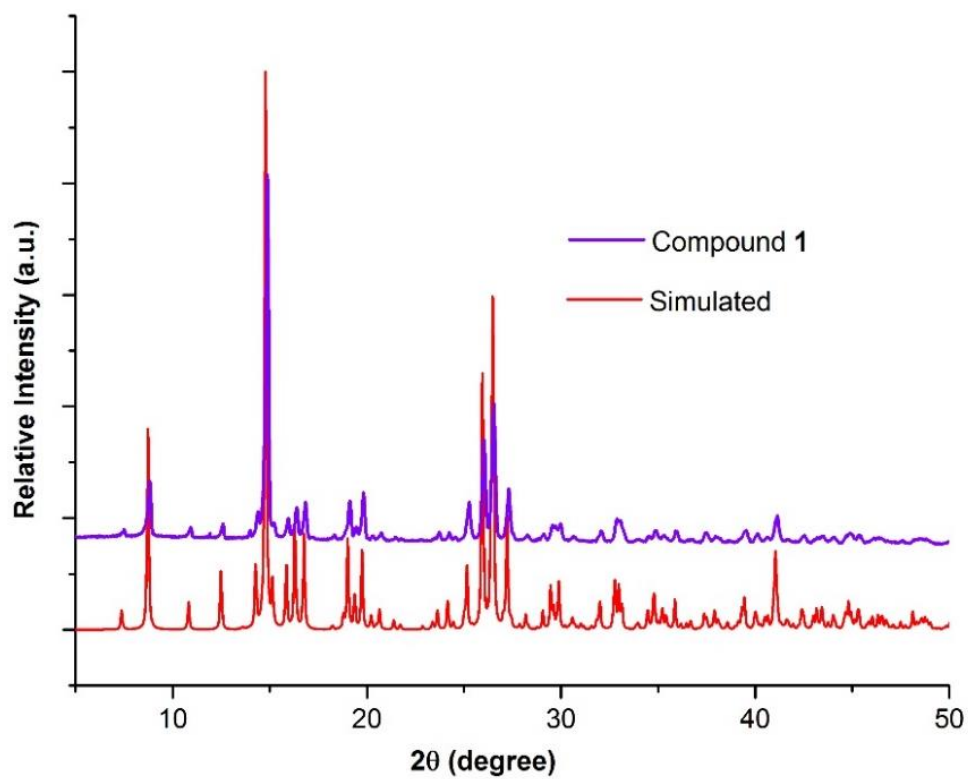


Figure S1. The Powder XRD pattern of compound **1** simulated (red in color) and experimental (violet in color).

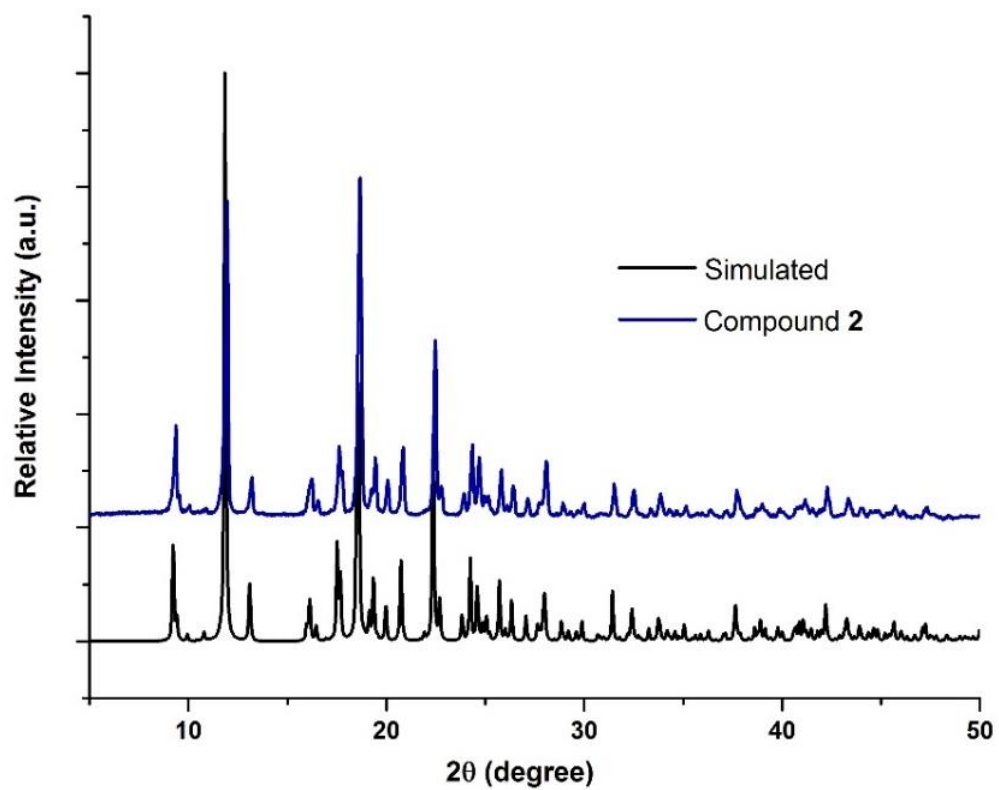


Figure S2. The Powder XRD pattern of compound **2** simulated (black in color) and experimental (blue in color).

(b) Thermogravimetric analysis (TGA)

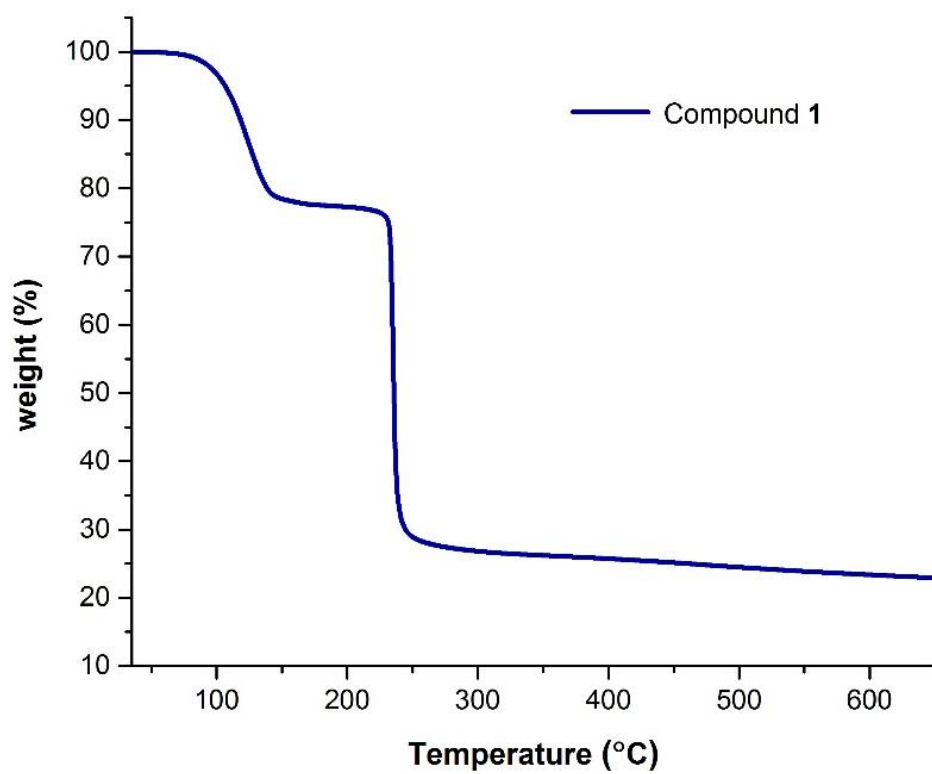


Figure S3. Thermogravimetric analysis plot of compound **1**.²

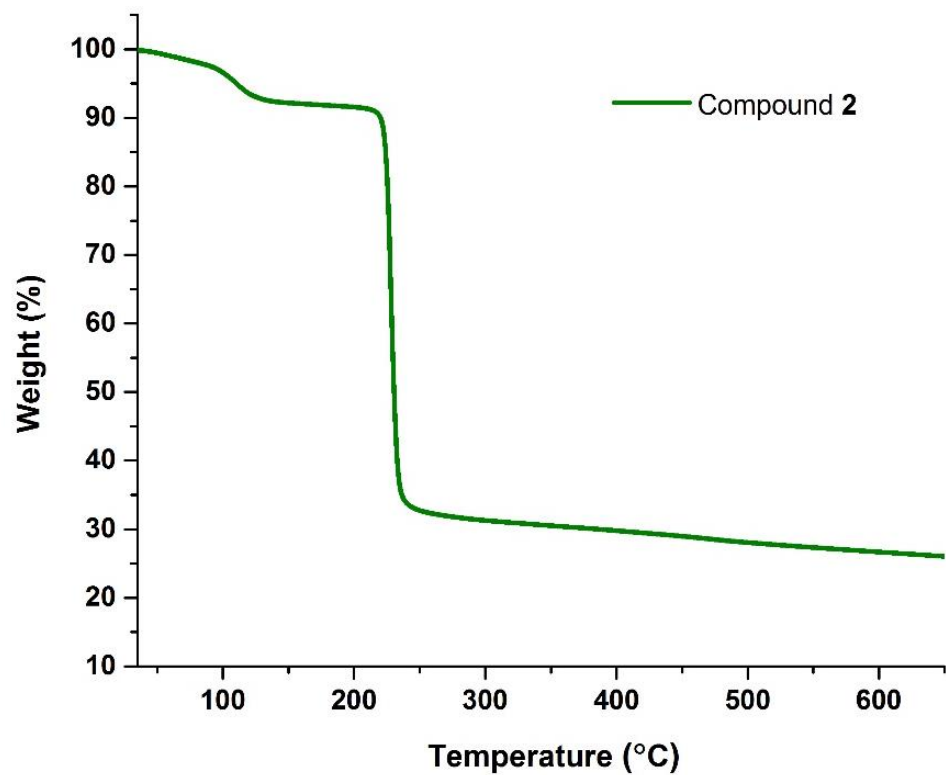


Figure S4. Thermogravimetric analysis plot of compound 2.

(c) Infrared (IR) spectroscopy studies

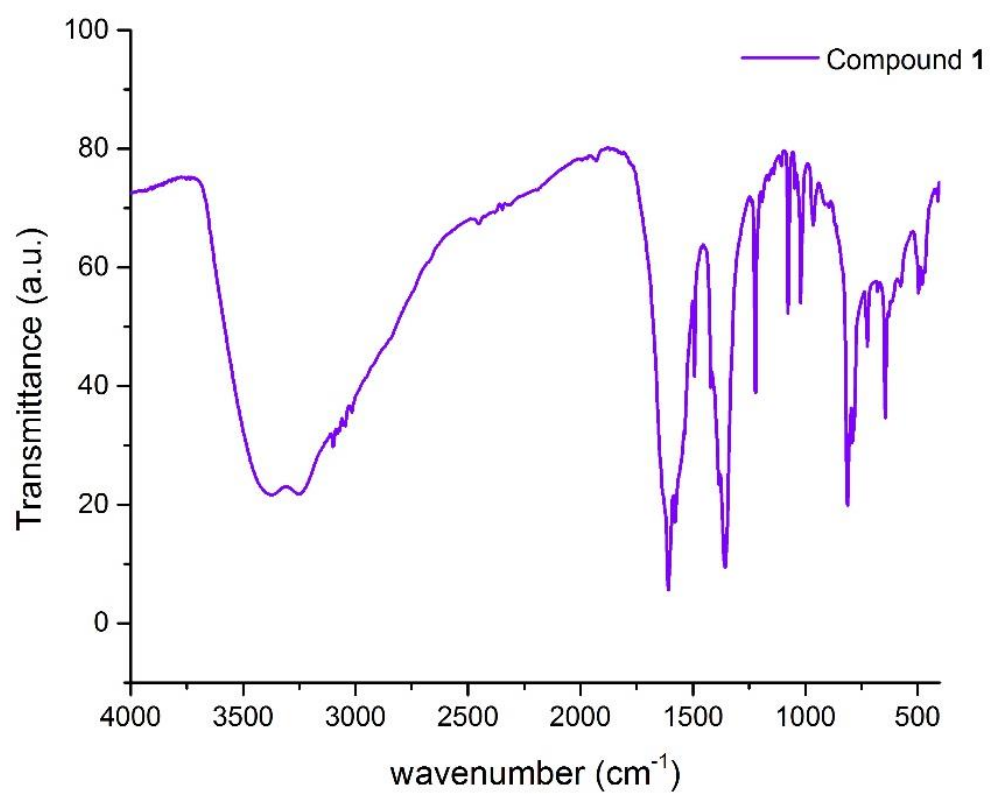


Figure S5. The IR plot of compound 1.

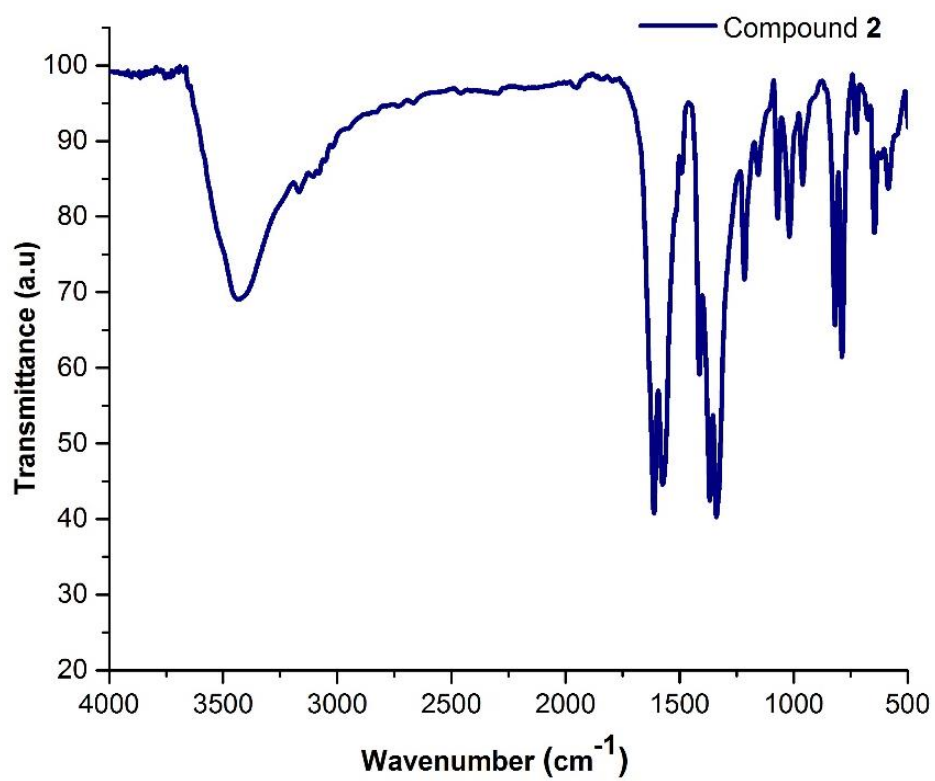


Figure S6. The IR plot of compound 2.

Solid-state circular dichroism (CD) measurements

Reference: KBr matrix

Sample: Compound **2** (crystals) and bulk powder

The crystals (and bulk powder) of compound **2** in 100 mg of dry KBr matrix were made in 10 mm diameter pellets using standard disk press. Then CD spectra were performed for pure KBr as a reference and the sample. The spectra were recorded for the wavelength range 200-800 nm for all the pellets with the path length of 1 nm. Here, we also measured CD spectra of crystals of compound **2** from three reaction vessels which were showing the same CD signal in all the cases.

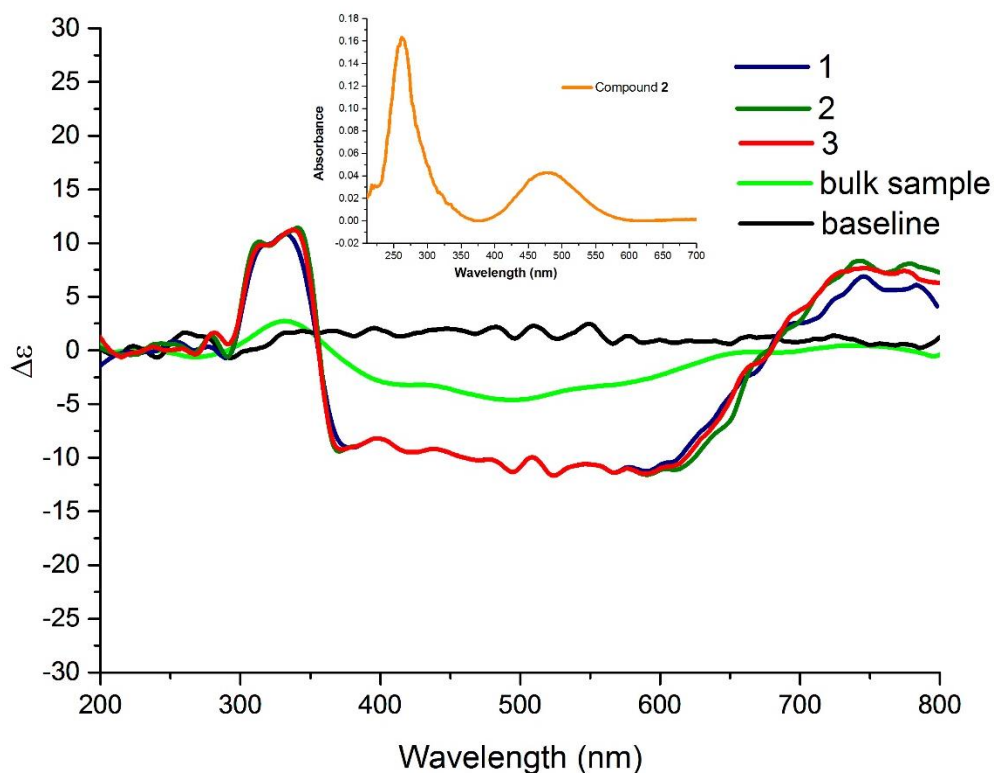


Figure S7. Solid-state circular dichroism (CD) spectra of crystals of compound **2** from three various reaction vials with reference (KBr matrix) and bulk powder samples. Inset shows solid-state UV-Visible absorption spectra of compound **2**.

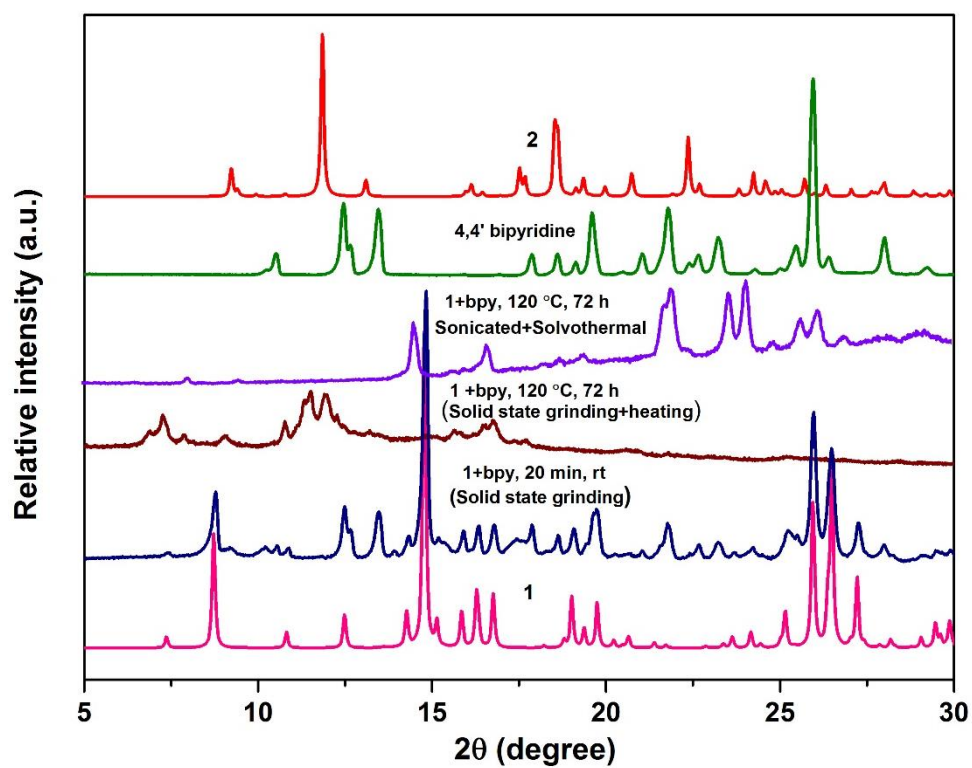


Figure S8. Several control experiments for the transformation of compound **1** to compound **2**.

Activation of compound **2**

The compound **2** was heated at 140 °C under vacuum for 3 h. After activation, material was maintained its crystallinity. The activation was confirmed by using TGA analysis, and crystallinity was observed by PXRD studies.

(a) Powder X-ray diffraction studies

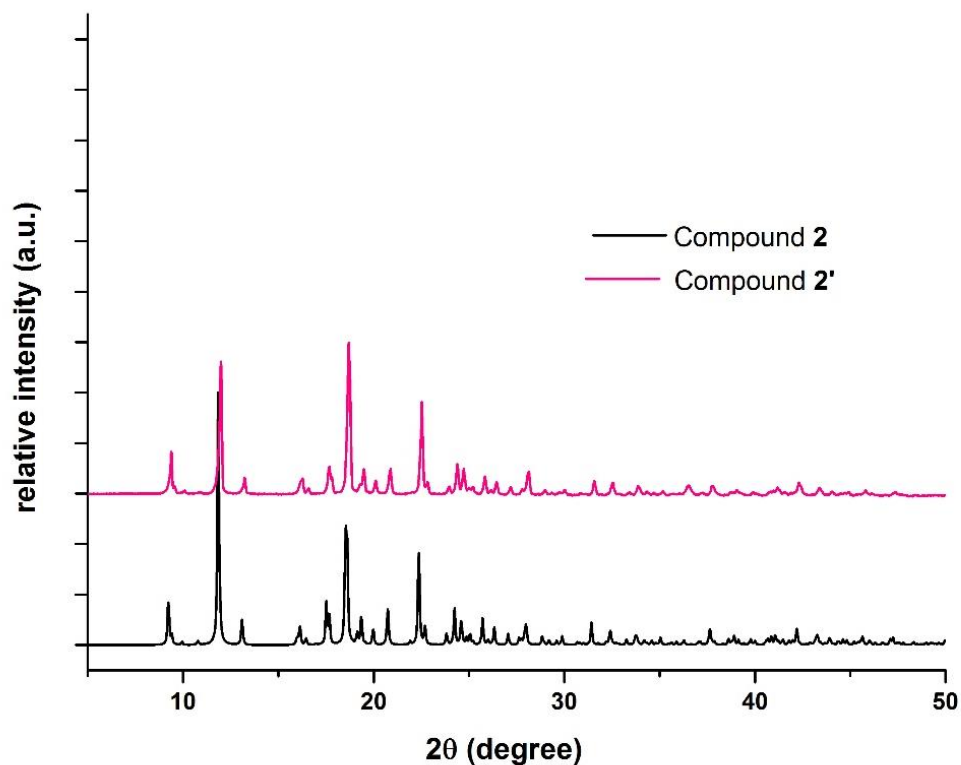


Figure S9. The PXRD pattern of compound **2** (black in color) and activated compound **2'** (pink in color).

(b) Thermogravimetric analysis (TGA)

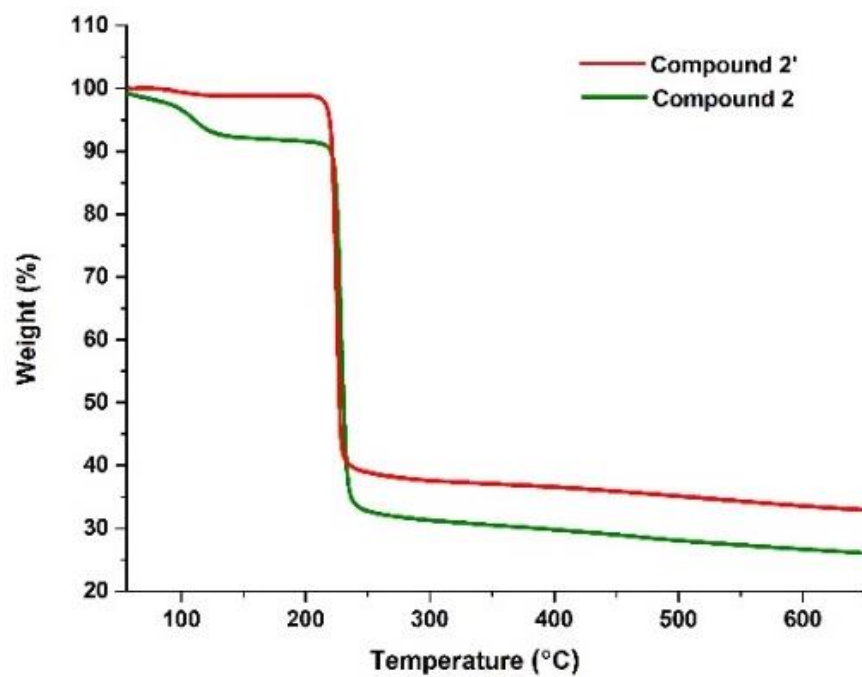


Figure S10. TGA plot of compound **2** (black in color) and activated compound **2'** (red in color).

Filtration Test

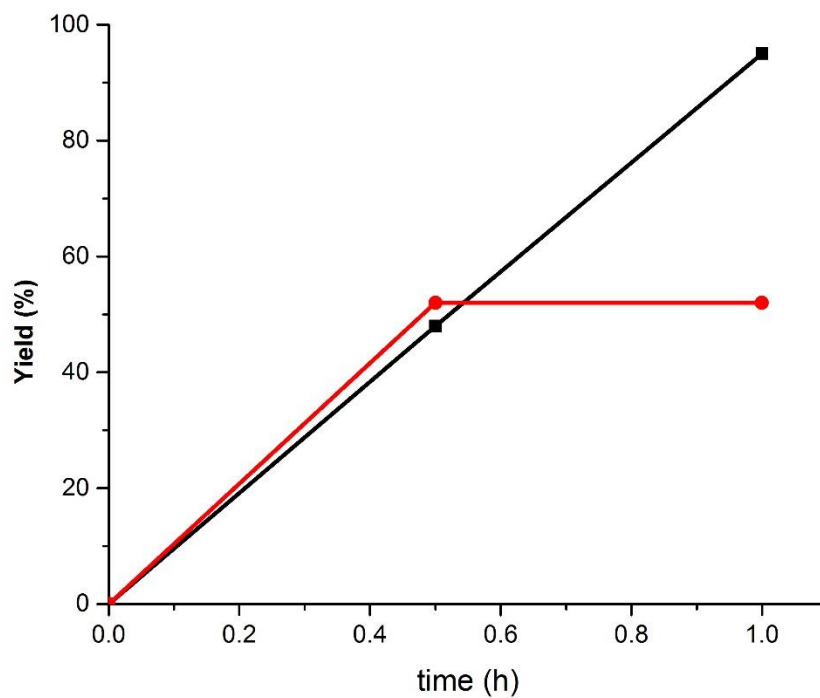


Figure S11. The enamine reaction after filtration of catalyst, there is no change in the yield of the product.

Recyclability test

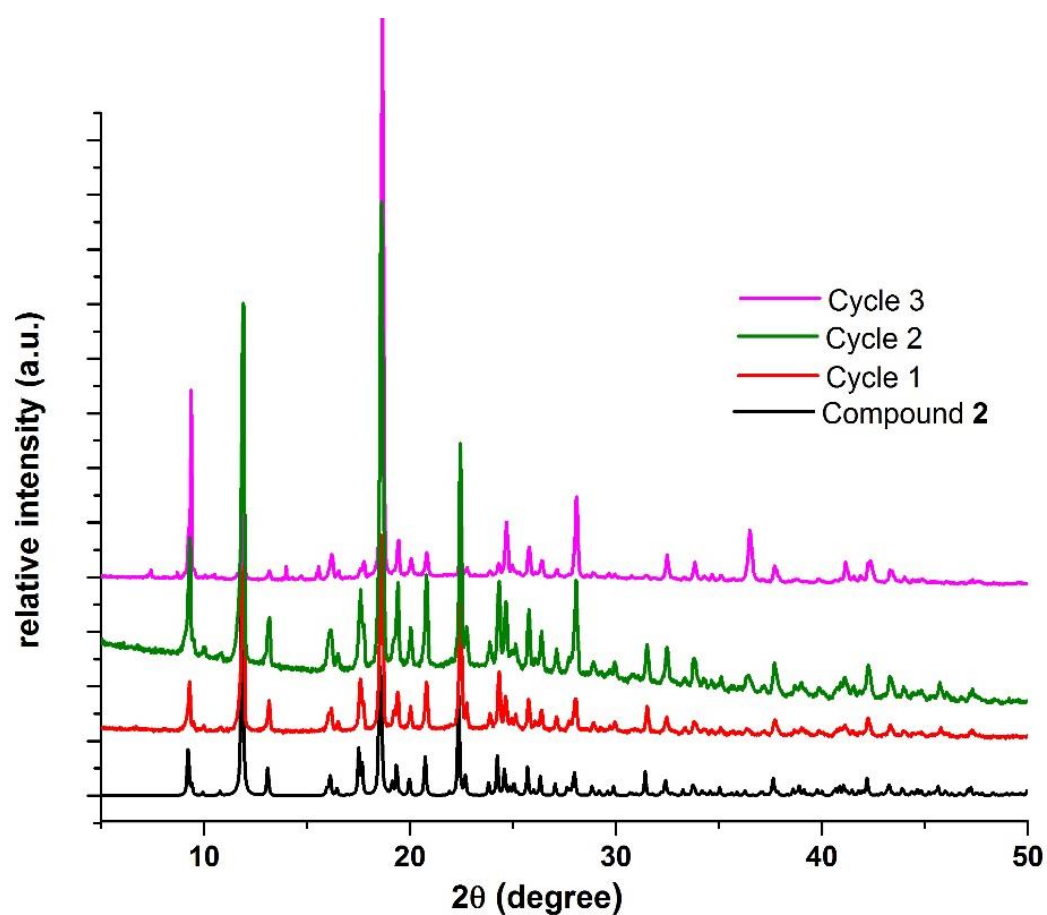


Figure S12. The powder X-ray diffraction patterns of reused catalyst (compound **2**) after each cycle of enamine reaction. It has shown that the structural integrity was maintained after each cycle.

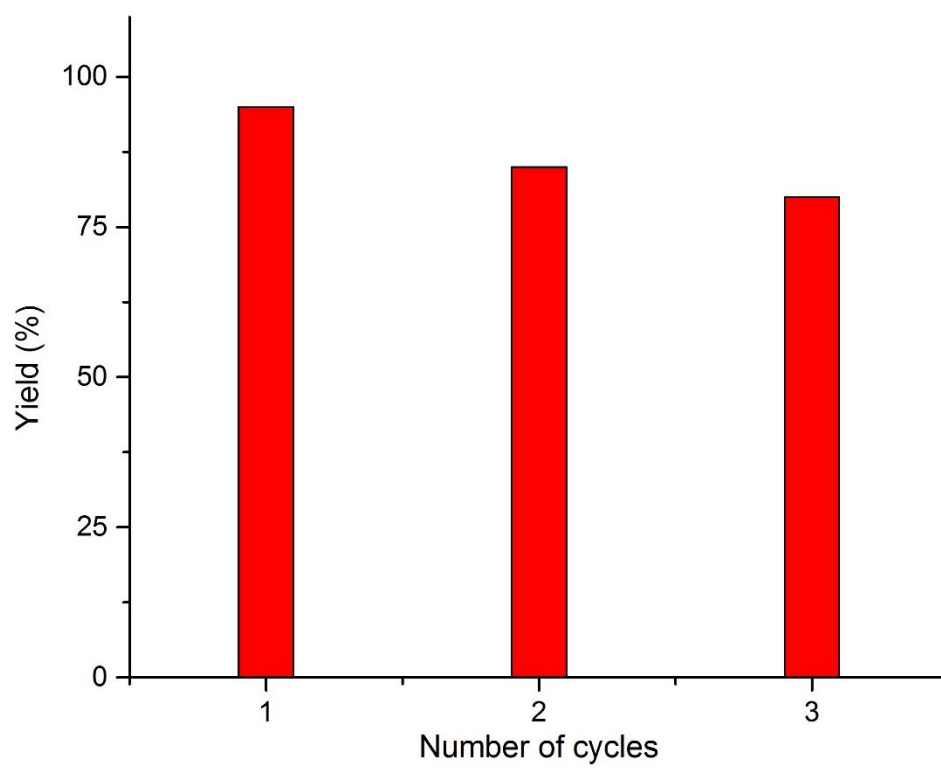


Figure S13. Recyclability bar diagram for enamine reaction.

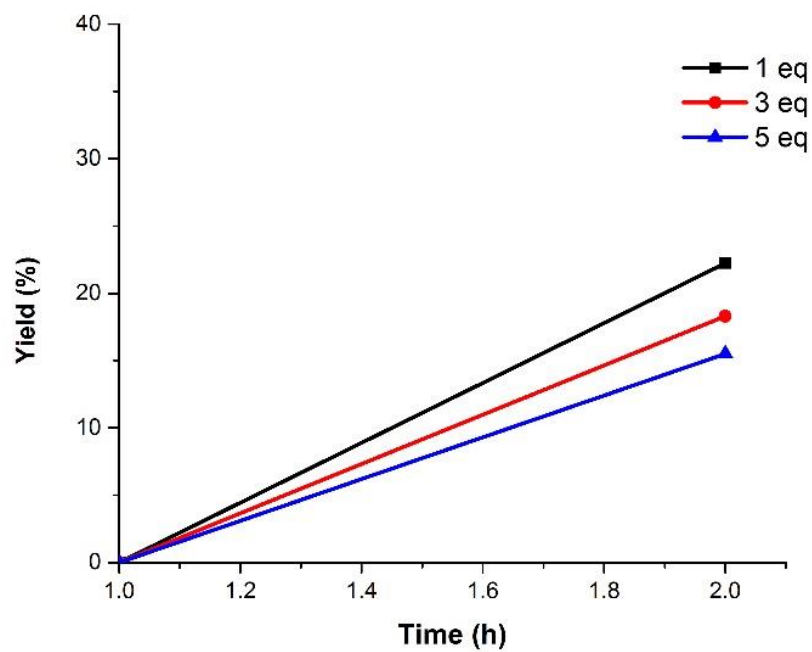


Figure S14. 1, 3 dipolar reaction was carried out at different concentrations of benzyl azide at 1, 3, 5 equivalents with respect to phenyl acetylene at various time intervals. (Catalyst used for the reaction was 5 mol% with respect to phenyl acetylene).

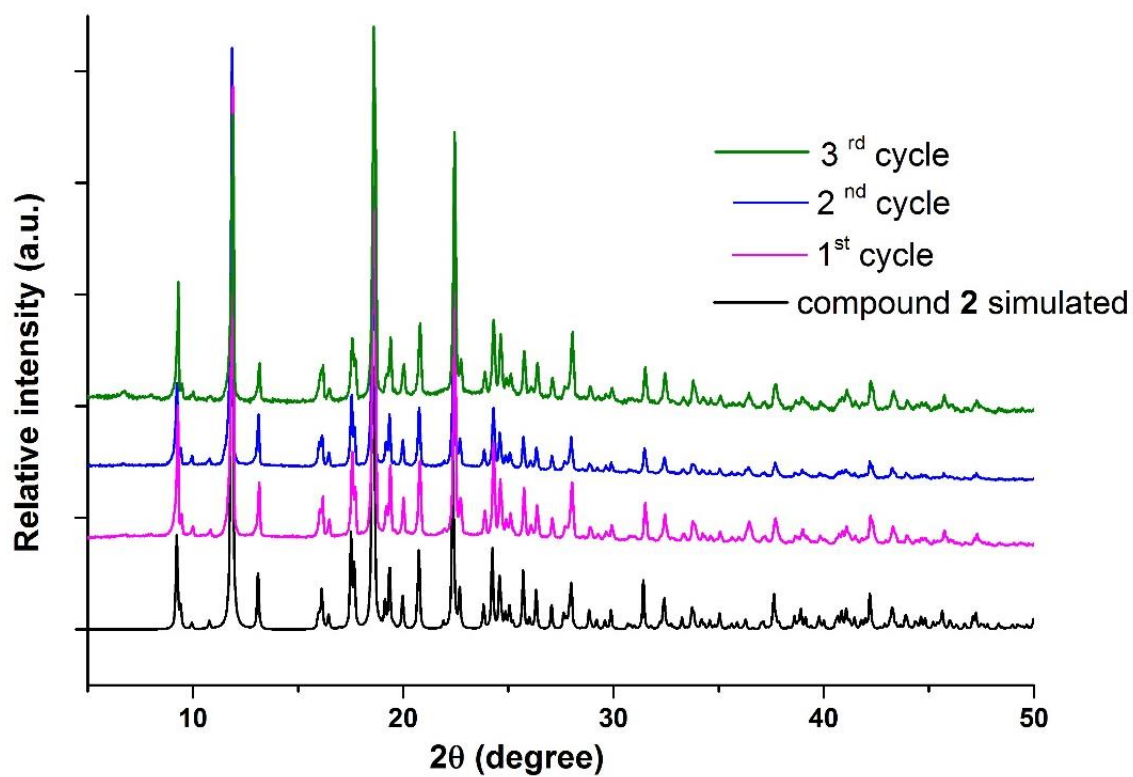
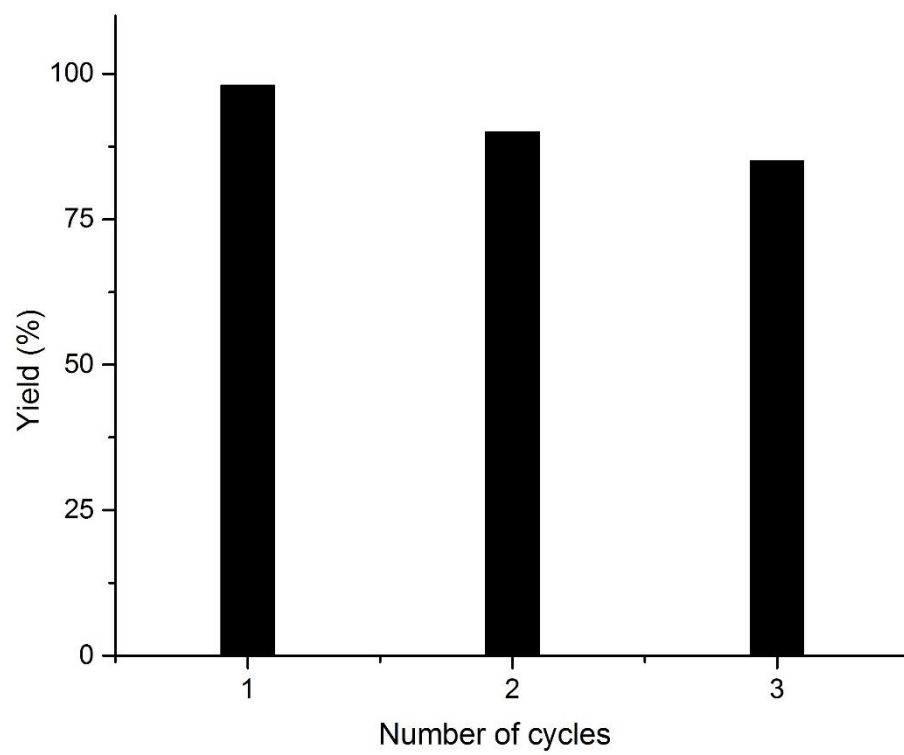


Figure S15. The powder X-ray diffraction patterns of reused catalyst (compound **2**) after each cycle of 1, 3 dipolar cycloaddition. It has shown that the structural integrity was maintained after each cycle.



3

Figure S16. Recyclability bar diagram for click reaction.

Leaching test

C:\SharedData\2016\CHEMISTRY\SKMPURNA\JUNE\01-06-16\CLICK-p-LEACH.spc

Label A:

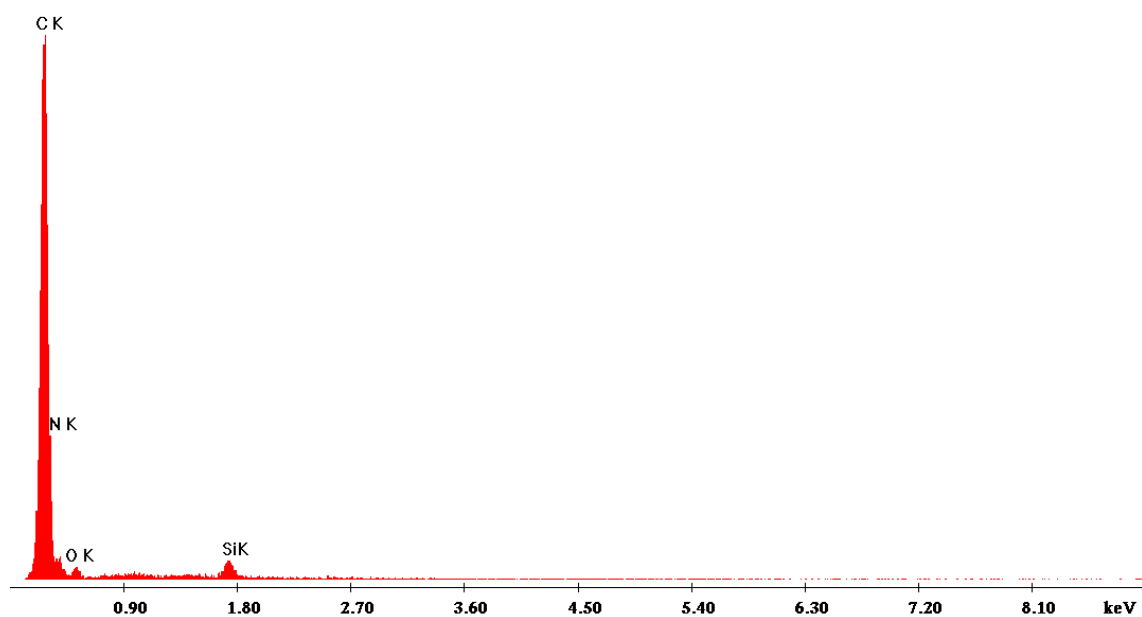


Figure S17. EDX analysis for leaching test for the click reaction.

References:

- (1) Yadav, J. S.; Kumar, V. N.; Rao, R. S.; Priyadarshini, A. D.; Rao, P. P.; Reddy, B. V. S.; Nagaiah, K. Sc(OTf)₃ catalyzed highly rapid and efficient synthesis of β -enamino compounds under solvent-free conditions. *J. Mol. Catal. A: Chem.* **2006**, 256, 234-237.
- (2) Zhang, Z.-H.; Yin, L.; Wang, Y.-M. A General and Efficient Method for the Preparation of β -Enamino Ketones and Esters Catalyzed by Indium Tribromide. *Adv. Synth. Catal.* **2006**, 348, 184-190.
- (3) Ramandeep, K. V.; Jean-Luc, R.; Bruneau, C. Efficient Synthesis of β -Aminoacrylates and β -Enaminones Catalyzed by Zn(OAc)₂·2H₂O. *Collect. Czech. Chem. Commun.* **2005**, 70, 1943-1952.